Segmentation and Restoration

Segmentation of echocardiographic images with Markov random fields

I. L. HERLIN[1], D. BEREZIAT[1], G. GIRAUDON[2], C. NGUYEN[1], C. GRAFFIGNE[3]

[1] INRIA, Rocquencourt
B.P. 105, 78153 Le Chesnay Cedex, France.
[2] INRIA Sophia-Antipolis
2004, route des Lucioles - B.P. 93
06902 Sophia Antipolis Cedex, France.
[3] Laboratoire de Mathématiques - Université Paris 11
Centre d'Orsay - Bâtiment 425
91405 Orsay Cedex, France.
Email: Isabelle.Herlin@inria.fr

Abstract. The aim of this work is to track specific anatomical structures in temporal sequences of echocardiographic images. This paper presents a new spatio-temporal model and describes the relevant spatial and temporal properties that must be taken into consideration to obtain the best possible results. It is expressed within a Markov random field framework and results are presented with different formulations of the temporal properties.

Keywords: Segmentation, Markov Random Field, Stochastic Process, Medical Images, Ultrasound.

1 Introduction

In [HNG92] a model of spatial segmentation for cardiac cavities in ultrasound images has been presented. This model supposes that grey level values of pixels, inside the cavity, follow a normal law parametrized by its constant mean and standard deviation. It supposes also that cavity's boundary includes a lot of points having a high gradient norm, and that the boundary is smooth. This model is sometimes insufficient and may produce inaccurate results; and we found necessary to define an another model [HG93], that includes temporal properties in three different ways: in the first place, we include a temporal neighborhood; secondly we use, inside the segmentation process, the result obtained on the previous image of the sequence; and thirdly we use a geometrical constraint on the stability of the cavity's center of mass. Again, this model presented some limitations and drawbacks, and this paper defines a new spatio-temporal model that takes two different types of motion into consideration: the cardiac boundaries are moving slowly during the cardiac cycle; the mitral valves are moving very fast.

Lecture Notes in Computer Science, Vol. 801
Jan-Olof Eklundh (Ed.)
Computer Vision – ECCV '94

Fig. 1 displays the echocardiographic video data and the cavity of interest in this study. These data were obtained on a VINGMED echograph from Henri Mondor Hospital, France (thanks to Gabriel Pelle). The sequence is 50 images and displays a cardiac cycle.

A major step in application of Gibbs fields or Markov fields to images viewed as two-dimensional arrays was D. and S. Geman's paper on image restoration [GG84]. The aim of the work presented here is non supervised segmentation based on a region growing algorithm [AG92], [Zuc76], and our paper is concerned with a special case of a region growing algorithm segmenting a cardiac cavity in ultrasound images.

2 Position of the problem

2.1 Description of the properties

This section is devoted to the description of the four main visual properties of a cardiac cavity scanned by ultrasound.

- homoneneity - The grey level values of the pixels inside the cavity are homogeneous. This property is translated into the following assumption: $\forall s \in C(x), im_s \sim \mathcal{N}(\mu_s, \sigma^2)$: the grey level value of each pixel of the cavity follows a normal law of local mean μ_s and constant standard deviation σ.
- smoothness - The second visual property concerns cavity's smoothness and boundary's smoothness. This property is expressed with an Ising model: the probability that a pixel is labelled 1, or -1, becomes higher if points in the neighborhood possess the same label.
- spatial gradient - The initial boundary of the cavity is attracted by high gradient norm values and the growing process must stop at the edge elements.
- temporal regularity - The result of segmentation presents a temporal regularity during the cardiac cycle.

2.2 Mathematical definition

We first define the following sets and variables:

- S denotes the set of pixels of the image; $\Gamma = \{0, \ldots, 255\}^{|S|}, \Omega = \{-1, 1\}^{|S|}$;
- $Im = (Im_s)_{s \in S}$ is a random variable defining the grey level values of the pixels. Its realization is $im = (im_s)_{s \in S} \in \Gamma$;
- $G = (G_s)_{s \in S}$ encodes the norm of the spatial gradient, $g = (g_s)_{s \in S} \in \Gamma$ and is obtained by Deriche's filter [Der87];
- $E = (E_s)_{s \in S}$ defines the edge process, $e = (e_s)_{s \in S} \in \Omega; e_s = 1 \Longleftrightarrow s$ is an edge element;
- $X = (X_s)_{s \in S}$ defines the segmentation process: $x = (x_s)_{s \in S} \in \Omega$ and $x_s = 1 \Longleftrightarrow s$ is inside the cavity; we denote by $C(x)$ the set of pixels inside this cavity;
- ν_s is the neighborhood of s (4-neighborhood);

- $y = (im, g, e)$ denotes the observation. It is the result of process $Y = (Im, G, E)$; x^0 is an initial segmentation for the cavity, used at the beginning of the optimization process.

3 Spatial properties

These properties were studied and compared in [HNG92, HG93]. The property 1 defines the first term of the energy function, which is minimized during the optimization process:

$$U_1(x,y) = \sum_{x \in C(x)} \left(\left(\frac{im_s - \mu_s}{\sigma} \right)^2 - T \right), \tag{1}$$

T being defined by the normal law table for a chosen percentage (95% or 99%).

Property 2 is expressed by an Ising Model and the second term of the energy function: $U_2(x) = -\alpha \sum_s x_s (\sum_{t \in \nu_s} x_t)$, α being a positive parameter.

Property 3 is included in the definition of μ_s. This local mean must express the fact that the grey level values become lower (i.e. darker) in the region of the cardiac muscle, where the gradient norm has high value: $\mu_s = \mu_0 + k g_s (1 - e_s)$. k being negative, the value of μ_s is decreasing from the center to the cavity's boundary.

4 Temporal properties

In [HG93] we made use of temporal information in different ways:

- To avoid escapes of the segmentation in the other cavity, when the mitral valve is open (see Fig. 1), we tried to add temporal properties and began with a first simple solution by adding a temporal neighborhood to the Ising model: $\nu'_s = \{\nu_s, s_{n-1}, s_{n+1}\}$ where ν_s is the spatial neighborhood and s_{n-1}, s_{n+1} are the pixels at same position than s on the previous image and on the next image of the sequence (n is the count of the studied image). The probability that a point is labelled 1 inside the cavity becomes higher if the pixel has the same label on the previous image or on the next image.
  This constraint is very strong and the segmentation result becomes too stable from an image to the next, as some modifications of the cavity are lost. On another hand, this temporal constraint is able to solve the problem of the opening of the mitral valve as shown on Fig. 2: the result of segmentation does not escape inside the other cavity.
- We suppose also that the position of the center of mass is not varying from an image to the next. This constraint is global and we approximate it by adding an isotropic constraint on the distance between each pixel of the cavity and the center of mass of the reference cavity (its coordinates are $(k_{\text{ref}}, l_{\text{ref}})$):

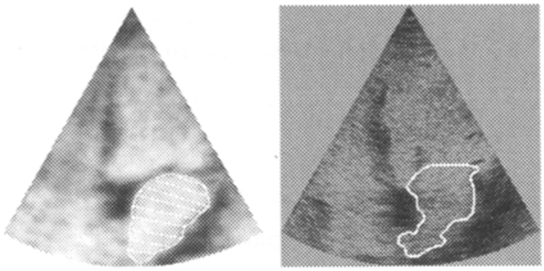

Fig. 1. **Left**: Echocardiographic video image and the studied cavity. **Right**: Mitral valves are opened: inaccuracy of segmentation

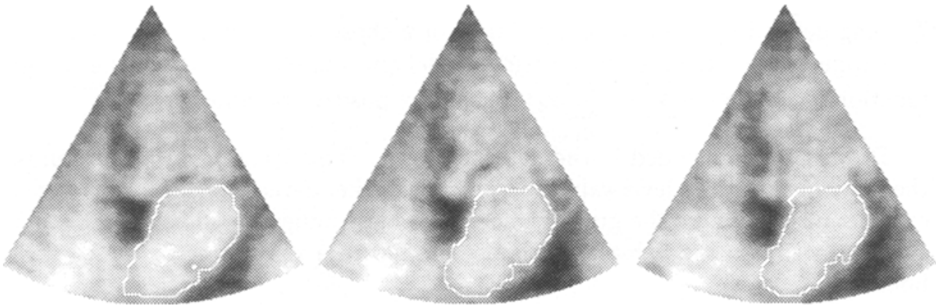

Fig. 2. Results of segmentation on three consecutive images of the sequence.

$\gamma \sum_{s \in C(x)} [(k_s - k_{\text{ref}})^2 + (l_s - l_{\text{ref}})^2 - dm^2]$ where (k_s, l_s) are the coordinates of s.

This energy term prevents a growing of the segmentation process in one particular direction. It avoids a penetration inside the other cavity if the mitral valve is open but, if pixels are nearer than dm, the label 1 is prefered.

In fact we need a temporal regularity constraint only in the region of the mitral valve because it is varying very fast.

In this region we have the following properties:

- the value of the spatial gradient (g_s) is low,
- the value of the temporal gradient (gt_s) is high.

At this point an energy term is added to help label -1 (outside the cavity) those pixels whose g_s term is low and gt_s high. In the same way all other configurations of g_s and gt_s help to label 1 (inside the cavity). In order to normalize the gradient values we make use of two functions, $\phi_c(g_s)$ and $\Psi_{c'}(gt_s)$ with values in $[0,1]$, such that $\phi_c(g_s) * \Phi_{c'}(gt_s)$ is maximum when g_s is low and gt_s is high.

These properties may be expressed by the global energy function:

$$U(x/y) = \sum_{s \in C(x)} \left[\left(\frac{im_s - \mu_s}{\sigma} \right)^2 - T \right] - \alpha \sum_{<s,t>} x_s x_t + \delta \sum_{s \in S} (\phi_c(g_s) * \Psi_{c'}(gt_s))$$

where ϕ_c and $\Psi_{c'}$ are two functions in $C^1(\mathbb{R}, [0,1])$ satisfying:

- $\phi_c(0) = 1; \phi_c(c) = 1/2; \lim_{x \to \infty} \phi_c(x) = 0;$
- $\Psi_{c'}(0) = 0; \Psi_{c'}(c) = 1/2; \lim_{x \to \infty} \Psi_{c'}(x) = 1.$

ϕ_c is a thresholding function of the high values of the spatial gradient and $\Psi_{c'}$ is a thresholding function of the low values of the temporal gradient.

With such a modelling, a point is labelled as inside the cavity if $\left(\frac{im_s - \mu_s}{\sigma}\right)^2 \leq t_{\text{loc}}$, with: $t_{\text{loc}} = T + 2\alpha \sum_{t \in \nu_s} x_t - 2\delta\phi_c(g_s) * \Psi_{c'}(gt_s)$. Now t_{loc} becomes very low in the region of the mitral valve and the growing process will stop because we impose $x_s = -1$ (outside the cavity) when reaching this region. The thresholding functions include a weighting coefficient δ that must verify the following property: if $(\phi_c(g_s) \simeq 1)$ and $(\Psi_{c'}(gt_s) \simeq 1)$ (i.e. low spatial gradient and high temporal gradient) we want to ensure that $\left(\frac{im_s - \mu_s}{\sigma}\right)^2 > t_{\text{loc}}$.

We studied this model with the following choices for ϕ_c and $\Psi_{c'}$:

- $\phi_c(x) = \frac{1-F(x/c)}{2}$, c is the mean of the norm of the spatial gradient,
- $\Psi_{c'}(x) = \frac{1+F(x/c')}{2}$, c' is the mean of the norm of the temporal gradient,
- $F(x) = \frac{1-x^a}{1+x^a}$, $a > 1$. The value of a allows to adjust the slope of the functions. We choose $a = 2$.

With these choices, we tested the model and concluded that:

- The results obtained with this model is approximately accurate, even if the mitral valve is open, as is shown on Fig. 3 (left).
- Moreover, the result are more stable regarding to the iteration count of the ICM algorithm. This is illustrated on Fig. 3 where the result with 5, 10 or 20 iterations of ICM are displayed from left to right. On the image on the right, we can observe penetrations in the borders of the mitral valve because the segmentation algorithm works with pixels with high gradient norm values inside the cavity.

5 Conclusion

In this paper, we have compared different mathematical translations of spatio-temporal properties used for segmentation. We have seen that making use of a local temporal neighborhood is too restrictive and that a global geometric

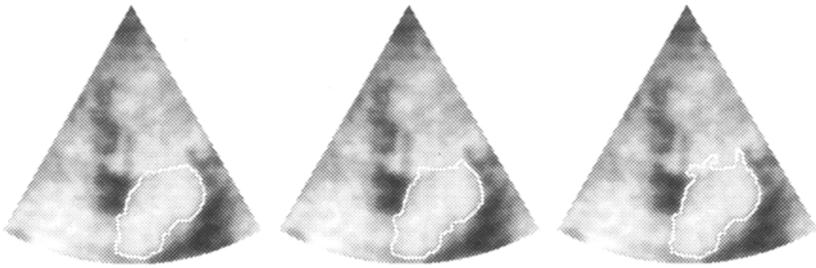

Fig. 3. Results of the model when the mitral valve is opened with 5, 10 and 20 ICM from left to right.

constraint on isotropy is accurate ; our final solution makes use of temporal gradient: this is a local constraint that takes into account all the images for recursive implementation. So we achieve the temporal tracking of a cardiac cavity during the cardiac cycle.

References

[AG92] R. Azencott and C. Graffigne. Non supervised segmentation using multi-level markov random fields. In *Proceedings of the 11th International Conference on Pattern Recognition*, August 30-September 3 1992.

[Der87] R. Deriche. Using Canny's criteria to derive a recursively implemented optimal edge detector. *International Journal of Computer Vision*, 1 (2), May 1987.

[GG84] S. Geman and D. Geman. Stochastic relaxation, Gibbs distribution and the Bayesian restoration of images. *IEEE Transactions on Pattern Analysis and Machine Intelligence*, 6:712–741, 1984.

[HG93] I. L. Herlin and G. Giraudon. Use of temporal information in a segmentation algorithm of ultrasound images. In *Proceedings of the conference on Computer Vision and Pattern Recognition*, New York, U.S.A., 15-17 June 1993.

[HNG92] I. Herlin, C. Nguyen, and C. Graffigne. Stochastic segmentation of ultrasound images. In *Proceedings of the 11th International Conference on Pattern Recognition*, August 30-September 3 1992.

[Zuc76] S.W. Zucker. Region growing: Childhood and adolescence. *Computer Graphics and Image Processing*, (5):382–399, 1976.